Global convergence of quorum-sensing networks

Giovanni Russo[1,*] and Jean Jacques E. Slotine[2,†]
[1]*Department of Systems and Computer Engineering, University of Naples Federico II, Napoli, Italy*
[2]*Nonlinear Systems Laboratory, Massachusetts Institute of Technology, Cambridge, Massachusetts 02139, USA*
(Received 30 May 2010; revised manuscript received 23 September 2010; published 25 October 2010)

In many natural synchronization phenomena, communication between individual elements occurs not directly but rather through the environment. One of these instances is bacterial quorum sensing, where bacteria release signaling molecules in the environment which in turn are sensed and used for population coordination. Extending this motivation to a general nonlinear dynamical system context, this paper analyzes synchronization phenomena in networks where communication and coupling between nodes are mediated by shared dynamical quantities, typically provided by the nodes' environment. Our model includes the case when the dynamics of the shared variables themselves cannot be neglected or indeed play a central part. Applications to examples from system biology illustrate the approach.

DOI: 10.1103/PhysRevE.82.041919 PACS number(s): 87.10.−e, 05.45.Xt

I. INTRODUCTION

Many dynamical phenomena in biology involve some form of *synchronization*. Synchronization has attracted much research both from the theoretical (see, e.g., [1–3] to cite just a few) and experimental [4,5] viewpoints. The particular case of synchronized *time-periodic* processes, where time scales can range from a few milliseconds to several years [6,7], includes, e.g., circadian rhythms in mammals [8], the cell cycle [9], spiking neurons [10], and respiratory oscillations [11].

When modeling such networks, it is often assumed that each node communicates directly with other nodes in the network (see, e.g., [12,13] and references therein). In many natural instances, however, network nodes do not communicate directly but rather by means of noisy and continuously changing environments. Bacteria, for instance, produce, release, and sense signaling molecules (the so-called autoinducers) which can diffuse in the environment and are used for population coordination. This mechanism, known as *quorum sensing* [14–16], is believed to play a key role in bacterial infection, as well as, e.g., in bioluminescence and biofilm formation [17,18]. In a neuronal context, a mechanism similar to that of quorum sensing may involve *local-field potentials*, which may play an important role in the synchronization of groups of neurons [19–26], or it may occur through a different level in a cortical hierarchy [27–31]. Other examples of such a mechanism are the synchronization of chemical oscillations of catalyst-loaded reactants in a medium of catalyst-free solution [32], cold atoms interacting with a coherent electromagnetic field [33], and the onset of coordinated activity in a population of microorganisms living in a shared environment [34,35].

From a network dynamics viewpoint, the key characteristic of quorum-sensing-like mechanisms lies in the fact that communication between nodes (e.g., bacteria) occurs by means of a shared quantity (e.g., the autoinducer concentration), typically in the environment. Furthermore, the production and degradation rates of such a quantity are affected by all the nodes of the network. Therefore, a detailed model of such a mechanism needs to keep track of the temporal evolution of the shared quantity, resulting in an additional set of ordinary differential equations. Such an indirect coupling model has been recently reported in, e.g., [36,37] in the context of periodic oscillations, while in [38] synchronization of two chaotic systems coupled through the environment is investigated. In these papers it is shown that under suitable conditions oscillators can synchronize and that this kind of coupling can lead to a rich variety of synchronous behaviors. In this paper, we will use the generic term "quorum sensing" to describe all such interactions through a shared environmental variable regardless of the dependence of this variable on the number of network nodes.

Mathematical work on such quorum-sensing topologies is relatively sparse (e.g., [21,36–40]) compared to that on diffusive topologies, and it often neglects the dynamics of the quorum variables or the environment, as well as the global effects of nonlinearities. This sparsity of results is somewhat surprising given that, besides its biological pervasiveness, quorum sensing may also be viewed as an astute "computational" tool. Specifically, the use of a shared variable in effect significantly reduces the number of links required to achieve a given connectivity [21].

This paper derives sufficient conditions for the coordination of nodes communicating through dynamical quorum-sensing mechanisms based on a full nonlinear dynamic analysis. These results can be used both to study natural networks and to guide design of communication mechanisms in synthetic or partially synthetic networks.

After introducing in Sec. II the basic mathematical tool used in the paper, we start with considering in Sec. III A the case where the network nodes (e.g., the biological entities populating the environment) are all identical or nearly identical. We then focus, in Sec. III B, on networks composed of heterogeneous nodes, i.e., nodes of possibly diverse dynamics. In this case we provide sufficient conditions ensuring that all the network nodes sharing the same dynamics converge to a common behavior, a particular instance of the so-called concurrent synchronization [41,42]. In Sec. III C,

*giovanni.russo2@unina.it
†jjs@mit.edu

the results are further extended to a distributed version of quorum sensing where multiple groups of possibly heterogeneous nodes communicate by means of multiple media. In Sec. IV, we show that driving the shared environmental variable with an exogenous signal of a given period provides a mechanism for making the network nodes oscillate at the same period, without requiring strong stability properties of the nodes or the overall system. Finally, Sec. V studies the dependence of synchronization properties on the number of nodes, a question of interest, e.g., in the context of cell proliferation. Section VI illustrates the general approach with a set of examples.

Our proofs are based on nonlinear contraction theory [43], a viewpoint on incremental stability which we briefly review in Sec. II and which has emerged as a powerful tool in applications ranging from Lagrangian mechanics to network control. Historically, ideas closely related to contraction can be traced back to [44] and even to [45] (see also [46], [47], and, e.g., [48] for a more exhaustive list of related references). As pointed out in [43], contraction is preserved through a large variety of system combinations, and in particular it represents a natural tool for the study and design of nonlinear state observers and, by extension, of synchronization mechanisms [49].

II. CONTRACTION THEORY TOOLS

A. Basic results

Recall that, given a norm $|\cdot|$ on the state space and its induced matrix norm $\|A\|$, for an arbitrary square matrix A, the associated *matrix measure* μ is defined as (see [50,51])

$$\mu(A) := \lim_{h\to 0^+} \frac{1}{h}(\|I+hA\|-1).$$

The basic result of nonlinear contraction analysis [43] which we shall use in this paper can be stated as follows.

Theorem 1. (Contraction). Consider the m-dimensional deterministic system

$$\dot{x} = f(x,t) \tag{1}$$

where f is a smooth nonlinear function. The system is said to be contracting if any two trajectories, starting from different initial conditions, converge exponentially to each other. A sufficient condition for a system to be contracting is the existence of some matrix measure, μ, such that

$$\exists \lambda > 0, \quad \forall \ x, \quad \forall \ t \geq 0, \quad \mu\left(\frac{\partial f(x,t)}{\partial x}\right) \leq -\lambda. \tag{2}$$

The scalar λ defines the contraction rate of the system.

The standard matrix measures used in this paper are listed in Table I. More generally, contraction may be shown by using matrix measures induced by the weighted vector norm $|x|_{\Theta,i}=|\Theta x|_i$, with Θ as a constant invertible matrix and $i=1,2,\infty$. Such measures, denoted with $\mu_{\Theta,i}$, are linked to the standard measures by

$$\mu_{\Theta,i}(A) = \mu_i(\Theta A \Theta^{-1}), \quad \forall \ i = 1,2,\infty.$$

TABLE I. Standard matrix measures for a real $n\times n$ matrix, $A := [a_{ij}]$. The ith eigenvalue of A is denoted with $\lambda_i(A)$.

Vector norm, $\lvert\cdot\rvert$	Induced matrix measure, $\mu(A)$
$\lvert x\rvert_1=\Sigma_{j=1}^n \lvert x_j\rvert$	$\mu_1(A)=\max_j(a_{jj}+\Sigma_{i\neq j}\lvert a_{ij}\rvert)$
$\lvert x\rvert_2=(\Sigma_{j=1}^n \lvert x_j\rvert^2)^{1/2}$	$\mu_2(A)=\max_i(\lambda_i\{\frac{A+A^*}{2}\})$
$\lvert x\rvert_\infty=\max_{1\leq j\leq n}\lvert x_j\rvert$	$\mu_\infty(A)=\max_i(a_{ii}+\Sigma_{j\neq i}\lvert a_{ij}\rvert)$

In this paper, Θ will be either the identity or a diagonal matrix. Note that for linear time-invariant systems, contraction is equivalent to strict stability, and, using the Euclidean vector norm, Θ can be chosen as the transformation matrix which diagonalizes the system or puts it in Jordan form [43].

For convenience, in this paper we will also say that a *function* $f(x,t)$ is contracting if the system $\dot{x}=f(x,t)$ satisfies the sufficient condition above. Similarly, we will then say that the corresponding Jacobian *matrix* $\frac{\partial f}{\partial x}(x,t)$ is contracting.

We shall also use the following two properties of contracting systems whose proofs can be found in [43,52].

Hierarchies of contracting systems. Assume that the Jacobian in Eq. (1) is in the form

$$\frac{\partial f}{\partial x}(x,t) = \begin{bmatrix} J_{11} & J_{12} \\ 0 & J_{22} \end{bmatrix}, \tag{3}$$

corresponding to a hierarchical dynamic structure. The J_{ii} may be of different dimensions. Then, a sufficient condition for the system to be contracting is that (i) the Jacobians J_{11} and J_{22} are contracting (possibly with different Θ's and for different matrix measures) and (ii) the matrix J_{12} is bounded.

Periodic inputs. Consider the system

$$\dot{x} = f(x,r(t)), \tag{4}$$

where the input vector $r(t)$ is periodic, of period T. Assume that the system is contracting [i.e., that the Jacobian matrix $\frac{\partial f}{\partial x}(x,r(t))$ is contracting for any $r(t)$]. Then, the system state $x(t)$ tends exponentially toward a periodic state of period T.

B. Partial contraction

A simple yet powerful extension to nonlinear contraction theory is the concept of *partial* contraction [49].

Theorem 2. (Partial contraction). Consider a smooth nonlinear m-dimensional system of the form $\dot{x}=f(x,x,t)$ and assume that the so-called virtual system $\dot{y}=f(y,x,t)$ is contracting with respect to y. If a particular solution of the auxiliary y system verifies a smooth specific property, then all trajectories of the original x system verify this property exponentially. The original system is said to be partially contracting.

Indeed, the virtual y system has two particular solutions, namely, $y(t)=x(t)$ for all $t\geq 0$ and the particular solution with the specific property. Since all trajectories of the y system converge exponentially to a single trajectory, this implies that $x(t)$ verifies the specific property exponentially.

C. Networks of contracting nodes

This section introduces preliminary results on concurrent synchronization of networks, which will be used in the rest of the paper.

We now consider a network where its $N>1$ nodes may have different dynamics (in the rest of the paper, we will say that nodes are heterogeneous),

$$\dot{x}_i = f_{\gamma(i)}(x_i,t) + \sum_{j\in N_i} [h_{\gamma(i)}(x_j) - h_{\gamma(i)}(x_i)], \tag{5}$$

where N_i denotes the set of neighbors of node i and γ is a function defined between two set of indices (not necessarily a permutation), i.e.,

$$\gamma:\{1,\ldots,N\} \to \{1,\ldots,s\} \quad s \leq N. \tag{6}$$

Thus, two nodes of Eq. (5), x_i and x_j, share the same dynamics and belong to the pth group (denoted with $\mathcal{G}_p$), i.e., $x_i, x_j \in \mathcal{G}_p$, if and only if $\gamma(i)=\gamma(j)=p$. The dimension of the nodes' state variables belonging to group p is $n_{\gamma(i)}$, i.e., $x_i \in \mathbb{R}^{n_{\gamma(i)}}$ for any $x_i \in \mathcal{G}_p$. In what follows we assume that the Jacobians of the coupling functions $h_{\gamma(i)}$ are diagonal matrices with non-negative diagonal elements. We will derive conditions ensuring *concurrent synchronization* in Eq. (5); i.e., all nodes belonging to the same group exhibit the same regime behavior.

In what follows the following standard assumption (see [41] and references therein) is made on the interconnections between the agents belonging to different groups [53].

Definition 1. Let i and j be two nodes of a group G_p, receiving their input from elements i' and j', respectively, with (i) i' and j' belonging to the same group $G_{p'}$, (ii) the coupling functions between i-i' and j-j' being the same, and (iii) the inputs to i and j coming from different groups are the same. If these assumptions are satisfied, then nodes i and j are said to be input equivalent.

Given this definition, we can state the following theorem, which generalizes results in [41] to the case of arbitrary norms. Its proof is provided in the Appendix.

Theorem 3. Assume that in Eq. (5) the nodes belonging to the same group are all input equivalent and that the node dynamics are all contracting. Then, all node trajectories sharing the same dynamics converge toward each other, i.e., for any x_i, $x_j \in \mathcal{G}_p$, $p=1,\ldots,s$,

$$|x_j(t) - x_i(t)| \to 0 \quad \text{as} \quad t \to +\infty.$$

In the case of networks of identical nodes dynamics, the above result amounts only to requiring contraction for each node.

III. MAIN RESULTS

In this section, we first provide sufficient conditions for the synchronization of a network composed of N nodes communicating over a common medium, itself characterized by some nonlinear dynamics. We then extend the analysis by providing sufficient conditions for the convergence of networks composed of nodes having different dynamics (nonhomogeneous nodes) or communicating over multiple (possibly nonhomogeneous) media.

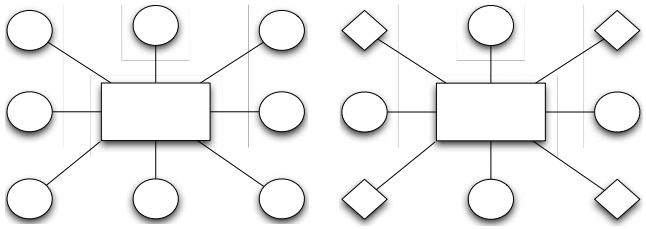

FIG. 1. A schematic representation of networks analyzed in Sec. III A (left) and Sec. III B (right). The nodes denoted with circles have a different dynamics from those indicated with squares. The dynamics of the common media is denoted with a rectangle. In our models, the dynamics of the common media is affected by the node state variables: this implements a feedback.

A. Basic mathematical model and convergence analysis

In the following, we analyze the convergent behavior of networks of nodes which are globally coupled through a shared quantity (often, the environment) [see Fig. 1 (left)]. In such a network, the N nodes are assumed be all identical, i.e., to share the same smooth dynamics and to communicate by means of the same common medium, also characterized by some smooth dynamics,

$$\dot{x}_i = f(x_i,z,t), \quad i=1,\ldots,N,$$

$$\dot{z} = g[z,\Psi(x_1,\ldots,x_N),t]. \tag{7}$$

A simplified version of the above model was recently analyzed by means of a graphical algorithm in [54]. In the above equation, the set of state variables of the nodes is x_i, while the set of the state variables of the common medium dynamics is z. Notice that the nodes dynamics and the medium dynamics can be of different dimensions (e.g., $x_i \in \mathbb{R}^n$, $z \in \mathbb{R}^d$). The dynamics of the nodes affect the dynamics of the common medium by means of some (coupling or input) function, $\Psi:\mathbb{R}^{Nn} \to \mathbb{R}^d$. These functions may depend only on some of the components of the x_i or of z (as the example in Sec. VI B illustrates).

The following result is a sufficient condition for convergence of all node trajectories in Eq. (7) toward each other.

Theorem 4. All node trajectories of network (7) globally exponentially converge toward each other if the function $f(x,v(t),t)$ is contracting for any $v(t) \in \mathbb{R}^d$.

Proof. The proof is based on partial contraction (Theorem 2). Consider the following *reduced order* virtual system,

$$\dot{y} = f(y,z,t). \tag{8}$$

Notice that now $z(t)$ is an exogenous input to the virtual system. Furthermore, substituting x_i to the virtual state variable y yields the dynamics of the ith node. That is, x_i, $i=1,\ldots,N$, are particular solutions of the virtual system. Now, if such a system is contracting, then all of its solutions will converge toward each other. Since the node state variables are particular solutions in Eq. (8), contraction of the virtual system implies that for any $i,j=1,\ldots,N$,

$$|x_i - x_j| \to 0 \quad \text{as} \quad t \to +\infty.$$

The Theorem is proved by noting that by hypotheses the function $f(x,v(t),t)$ is contracting for any exogenous input $v(t)$. This, in particular, implies that $f(y,z,t)$ is contracting; i.e., Eq. (8) is contracting. □

Remarks.

(a) In the case of diffusivelike coupling between nodes and the common medium, system (7) is reduced to

$$\dot{x}_i = f(x_i,t) + k_z(z) - k_x(x_i) \quad i = 1, \ldots, N,$$

$$\dot{z} = g(z,t) + \sum_{i=1}^{N} [u_x(x_i) - u_z(z)]. \tag{9}$$

That is, the nodes and the common medium are coupled by means of the smooth functions $k_z: \mathbb{R}^d \to \mathbb{R}^n$, $k_x: \mathbb{R}^n \to \mathbb{R}^n$ and $u_x: \mathbb{R}^n \to \mathbb{R}^d$, $u_z: \mathbb{R}^d \to \mathbb{R}^d$. These functions may depend only on some of the components of the x_i or z (as we shall illustrate in Sec. VI B). Theorem 4 implies that synchronization is attained if $f(x,t) - k_x(x)$ is contracting. Similar results are easily derived for the generalizations of the above model presented in what follows.

(b) The result also applies to the case where the quorum signal is based not on the x_i's themselves but rather on variables derived from the x_i's through some further nonlinear dynamics. Consider, for instance, the system

$$\dot{x}_i = f(x_i,z,t), \quad i = 1, \ldots, N,$$

$$\dot{r}_i = h(r_i,x_i,z,t), \quad i = 1, \ldots, N,$$

$$\dot{z} = g[z, \Psi(r_1, \ldots, r_N), t].$$

Theorem 4 can be applied directly by describing each network node by the augmented state (x_i, r_i) and using property (3) on hierarchical combinations to evaluate the contraction properties of the augmented network dynamics.

(c) Similarly, each network "node" may actually be composed of several subsystems, with each subsystem synchronizing with its analogs in other nodes.

(d) As in previous contraction work, the individual node dynamics are quite general and could describe, e.g., neuronal oscillator models as well as biochemical reactions. In the case that the individual node dynamics represents a system with multiple equilibria, then synchronization corresponds to a common "vote" for a particular equilibrium.

(e) A condition for synchronization weaker than Theorem 4 is that the function $f(x,v,t)$ be contracting only for some values of v, i.e., $v \in V \subset \mathbb{R}^d$. In this case, the medium dynamics acts as a switch which activates or deactivates synchronization according to the values of z.

B. Multiple systems communicating over a common medium

We now generalize the mathematical model analyzed in Sec. III A by allowing for $s \leq N$ groups (or clusters) of nodes characterized by different dynamics (with possibly different dimensions) to communicate over the same common medium (see Fig. 1, right). We will prove a sufficient condition for the global exponential convergence of all node trajectories belonging to the same group toward each other. This regime is called concurrent synchronization [41].

The mathematical model analyzed here is

$$\dot{x}_i = f_{\gamma(i)}(x_i,z,t),$$

$$\dot{z} = g[z, \Psi(x_1, \ldots, x_N), t], \tag{10}$$

where (i) γ is defined as in Eq. (6), (ii) x_i denotes the state variables of the network nodes (nodes belonging to different groups may have different dimensions, say $n_{\gamma(i)}$) and z denotes the state variables for the common medium ($z \in \mathbb{R}^d$); and (iii) Ψ, defined analogously in Sec. III A, denotes the coupling function of the group $\gamma(i)$ with the common medium dynamics ($\Psi: \mathbb{R}^{n_{\gamma(1)}} \times \cdots \times \mathbb{R}^{n_{\gamma(N)}} \to \mathbb{R}^d$).

Theorem 5. Concurrent synchronization is achieved in network (10) if the functions $f_{\gamma(i)}(x,v(t),t)$ are all contracting for any $v(t) \in \mathbb{R}^d$.

Proof. Recall that Eq. (10) is composed by N nodes having dynamics $f_1, \ldots, f_s$. Now, in analogy with the proof of Theorem 4, consider the following virtual system:

$$\dot{y}_1 = f_1(y_1,z,t),$$

$$\dot{y}_2 = f_2(y_2,z,t),$$

$$\vdots$$

$$\dot{y}_s = f_s(y_s,z,t), \tag{11}$$

where $z(t)$ is seen as an exogenous input to the virtual system. Let $\{X_i\}$ be the set of state variables belonging to the ith group composing the network and denote with $X_{i,j}$ any element of $\{X_i\}$. We have $(X_{1,j}, \ldots, X_{s,j})$ as the particular solutions of the virtual system. Now, contraction of the virtual system implies that all of its particular solutions converge toward each other, which in turn implies that all the elements within the same group $\{X_i\}$ converge toward each other. Thus, contraction of virtual system (11) implies concurrent synchronization of real system (10).

To prove contraction of Eq. (11), compute its Jacobian,

$$J = \begin{bmatrix} \frac{\partial f_1(y_1,z,t)}{\partial y_1} & 0 & 0 & \ldots & 0 \\ 0 & \frac{\partial f_2(y_2,z,t)}{\partial y_2} & 0 & \ldots & 0 \\ \ldots & \ldots & \ldots & \ldots & \ldots \\ 0 & 0 & 0 & 0 & \frac{\partial f_s(y_s,z,t)}{\partial y_s} \end{bmatrix}.$$

Now, by hypotheses, we have that all the functions $f_i(x,v(t),t)$ are contracting for any exogenous input. This, in turn, implies that virtual system (11) is contracting since its Jacobian matrix is block diagonal with diagonal blocks being contracting. □

C. Systems communicating over different media

In Sec. III B, we considered networks where some (possibly heterogeneous) nodes communicate over a common

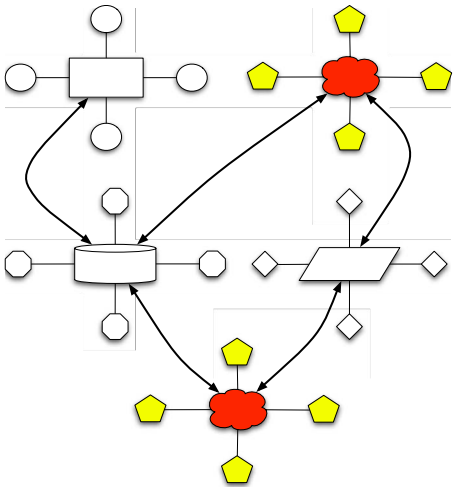

FIG. 2. (Color online) A schematic representation of the network analyzed Sec. III C. The connections between media (and hence the connections of the autonomous level) are pointed out. Notice that only two nodes of the autonomous level are input equivalent (also pointed out in the figure) since (i) their media have the same dynamics and (ii) both media are shared by the same number of nodes which have the same dynamics.

medium. We now consider a *distributed* version of such topology, where each of the $s \leq N$ groups composing the network has a private medium. Communication between the groups is then obtained by coupling only their media (see Fig. 2). The objective of this section is to provide a sufficient condition ensuring (concurrent) synchronization of such network topology.

Note that the network topology considered here presents a layer structure. In analogy with the terminology used for describing the topology of the Internet and the World Wide Web (see, e.g., [55,56]), we term as *medium* (or private) level the layer consisting of the nodes of the network and their corresponding (private) media; we then term as *autonomous* level the layer of the interconnections between the media. That is, the autonomous level is an *abstraction* of the network, having nodes which consist of both the network nodes and their private medium. This in turn implies that in order for two nodes of the autonomous level to be identical they have to share (i) the same dynamics and number of nodes and (ii) the same medium dynamics (see Fig. 2).

In what follows we will denote with $\mathcal{G}_p$ the set of homogeneous nodes communicating over the medium z_p. We will denote with N_p the set of media which are linked to the medium z_p. Each medium communicates with its neighboring media diffusively. The mathematical model is then

$$\dot{x}_i = f_p(x_i, z_p, t), \quad x_i \in \mathcal{G}_p,$$

$$\dot{z}_p = g_p(z_p, \Psi(X_p), t) + \sum_{j \in N_p} [\phi_p(z_j) - \phi_p(z_p)], \quad x_i \in \mathcal{G}_p, \tag{12}$$

where $p = 1, \ldots, s$ and X_p is the stack of all the vectors $x_i \in \mathcal{G}_p$. We assume that the dynamical equations for the media have all the same dimensions (e.g., $z_p \in R^d$), while the nodes belonging to different groups can have different dimensions (e.g., $x_i \in \mathbb{R}^p$ for any $i \in \mathcal{G}_p$). Here, the coupling functions between the media, $\phi_p : \mathbb{R}^d \to \mathbb{R}^d$, are assumed to be continuous and to have a diagonal Jacobian matrix with diagonal elements being non-negative and bounded. All the matrices $\partial f_p / \partial z$ are assumed to be bounded.

Theorem 6. Concurrent synchronization is attained in network (12) if (i) the nodes of its autonomous level sharing the same dynamics are input equivalent, (ii) $f_p(x_i, v(t), t)$ and $g_p(z_p, v(t), t)$ are all contracting functions for any $v(t) \in \mathbb{R}^d$, and (iii) $\partial f_p / \partial z_p$ are all uniformly bounded matrices.

Proof. Consider the following two-dimensional virtual system analogous to the one used for proving Theorem 5,

$$\dot{y}_{1,p} = f_p(y_{1,p}, y_{2,p}, t),$$

$$\dot{y}_{2,p} = g_p(y_{2,p}, v_p(t), t) + \sum_{k \in N_p} [\phi_p(y_{2,k}) - \phi_p(y_{2,p})], \tag{13}$$

where $p = 1, \ldots, s$ and $v_p(t) := \Psi(X_p)$. Notice that the above system is constructed in a similar way as in Eq. (11). In particular, solutions of Eq. (12) are particular solutions of the above virtual system (see the proof of Theorem 5). That is, if concurrent synchronization is attained for Eq. (13), then all the nodes sharing the same dynamics will converge toward each other. Now, Theorem 3 implies that concurrent synchronization is attained for system (13) if (i) its nodes are contracting, (ii) the coupling functions have a non-negative bounded diagonal Jacobian, and (iii) nodes sharing the same dynamics are input equivalent. Since the last two conditions are satisfied by hypotheses, we only have to prove contraction of the virtual network nodes. Differentiation of node dynamics in Eq. (13) yields the Jacobian matrix

$$\begin{bmatrix} \dfrac{\partial f_p(y_{1,p}, y_{2,p}, t)}{\partial y_{1,p}} & \dfrac{\partial f_p(y_{1,p}, y_{2,p}, t)}{\partial y_{2,p}} \\ 0 & \dfrac{\partial g_p(y_{1,p}, v_i(t), t)}{\partial y_{2,p}} \end{bmatrix}.$$

The above Jacobian has the structure of a hierarchy. Thus (see Sec. II), the virtual system is contracting if (i) $\partial f_p(y_{1,p}, y_{2,p}, t) / \partial y_{1,p}$ and $\partial g_p(y_{2,p}, v_i(t), t) / \partial y_{2,p}$ are both contracting and (ii) $\partial f_p(y_{1,p}, y_{2,p}, t) / \partial y_{2,p}$ is bounded.

The above two conditions are satisfied by hypotheses. Thus, the virtual network achieves concurrent synchronization (Theorem 3). This proves the theorem. □

Note that Theorems 4 and 5 do not make any hypotheses on the medium dynamics—synchronization (or concurrent synchronization) can be attained by the network nodes independently of the particular dynamics of the single medium, provided that the function f (or the f_i's) is contracting. By contrast, Theorem 6 shows that the media dynamics becomes a key element for achieving concurrent synchronization in networks where different groups communicate over different media.

Finally, note that all of the above results also allow dimensionality reduction in the analysis of the system's final behavior by treating each group as a single element, similarly to [57], a point we will further illustrate in Sec. V.

IV. CONTROL OF PERIODICITY

The objective of this section is to provide a sufficient condition to guarantee that the common node behavior toward which all network nodes globally converge is oscillatory and exhibits a specified *period*. This is obtained by driving the environmental dynamics with an exogenous signal of the given period. A related problem has been recently addressed in [58] where entrainment of individual contracting biological systems to periodic inputs was analyzed. In our context, the result is by no means a direct application of the theorem on entrainment of contracting systems to periodic inputs discussed in Sec. II A, as the nodes or the overall system need not be contracting and thus the role of the bilateral interaction between nodes and shared environmental variable becomes central.

Our main result, which we shall extend later in the section, is as follows.

Theorem 7. Consider the following network:

$$\dot{x}_i = f(x_i, z, t), \quad i = 1, \ldots, N,$$

$$\dot{z} = g[z, \Psi(x_1, \ldots, x_N), t] + r(t), \tag{14}$$

where $r(t)$ is a T-periodic signal. All the nodes of the network synchronize onto a periodic orbit of period T if (i) $f(x_i, v(t), t)$ and $g(z, v(t), t)$ are contracting functions for any $v(t) \in \mathbb{R}^d$ and (ii) $\frac{\partial f}{\partial z}$ is bounded.

Note that the dynamics f and g include the coupling terms between nodes and environment.

Proof. Consider the virtual system

$$\dot{y}_1 = f(y_1, y_2, t),$$

$$\dot{y}_2 = g(y_2, v(t), t) + r(t), \tag{15}$$

where $v(t) \coloneqq \Psi(x_1, \ldots, x_N)$. We will prove the theorem by showing that such a system is contracting. Indeed, in this case, the trajectories of Eq. (15) will globally exponentially converge to a unique T-periodic solution, implying that also x_i will exhibit a T-periodic final behavior. It is straightforward to check that differentiation of the virtual system yields a matrix of form (3). That is, the virtual system is a hierarchy and thus (see Sec. II) it is contracting if (i) $\partial f(y_1, y_2, t)/\partial y_1$ and $\partial g(y_2, v(t), t)/\partial y_2$ are both contracting and (ii) $\partial f(y_1, y_2, t)/\partial y_2$ is bounded.

The first condition is satisfied since, by hypotheses, the functions $f(x, v(t), t)$ and $g(z, v(t), t)$ are contracting for any $v \in \mathbb{R}^d$. The second condition is also satisfied since we assumed $\partial f/\partial z$ to be bounded. The Theorem is then proved. □

System (14) can be thought of as a dynamical system built upon a bidirectional interaction between nodes and medium and forced by a periodic input. In this view, the conditions of Theorem 7 guarantee global exponential synchronization of the network nodes onto a periodic orbit of the same period as the input, without requiring contraction of either the nodes or the overall dynamics. Indeed, the proof of the theorem is based on contraction of an appropriately constructed *virtual* system, a much weaker condition. In this sense, our result provides a generalization of the basic result on global entrainment to periodic inputs discussed in Sec. II A.

Theorem 7 can be extended to the more general case of networks of nonhomogeneous nodes communicating over nonhomogeneous media.

Theorem 8. Consider the following network:

$$\dot{x}_i = f_p(x_i, z_p, t), \quad x_i \in \mathcal{G}_p,$$

$$\dot{z}_p = g_p[z_p, \Psi(X_p), t] + \sum_{k \in N_p} [\phi(z_k) - \phi(z_p)] + r(t) \quad x_j \in \mathcal{G}_p, \tag{16}$$

where X_p is the stack of all the $x_i \in \mathcal{G}_p$ and $r(t)$ is a T-periodic signal. Concurrent synchronization is attained, with a final behavior periodic behavior of period T if

(1) the nodes of the autonomous level sharing the same dynamics are input equivalent;

(2) the coupling functions ϕ have bounded diagonal Jacobian with non-negative diagonal elements;

(3) $f_p(x_i, v(t), t)$ and $g_p(z_p, v(t)t)$ are contracting functions for any $v(t) \in \mathbb{R}^d$; and

(4) $\partial f_p/\partial z_p$ are all uniformly bounded matrices.

Proof. The proof is formally the same as that of Theorem 6 and Theorem 7, and it is omitted here for the sake of brevity. □

Simple example

Consider a simple biochemical reaction, consisting of a set of $N > 1$ enzymes sharing the same substrate. We denote with $X_1, \ldots, X_N$ the concentration of the reaction products. We also assume that the dynamics of S is affected by some T-periodic input, $r(t)$. We assume that the total concentration of X_i, i.e., $X_{i,T}$, is much less than the initial substrate concentration, S_0. In these hypotheses, a suitable mathematical model for the system is given by (see, e.g., [59])

$$\dot{X}_i = -aX_i + \frac{K_1 S}{K_2 + S}, \quad i = 1, \ldots, N,$$

$$\dot{S} = -\sum_{i=1}^{N} \frac{K_1 S}{K_2 + S} + r(t). \tag{17}$$

with K_1 and K_2 as positive parameters. Thus, a suitable virtual system for the network is

$$\dot{y}_1 = -ay_1 + \frac{K_1 y_2}{K_2 + y_2},$$

$$\dot{y}_2 = -\sum_{i=1}^{N} \frac{K_1 y_2}{K_2 + y_2} + r(t). \tag{18}$$

Differentiation of the above system yields the Jacobian matrix

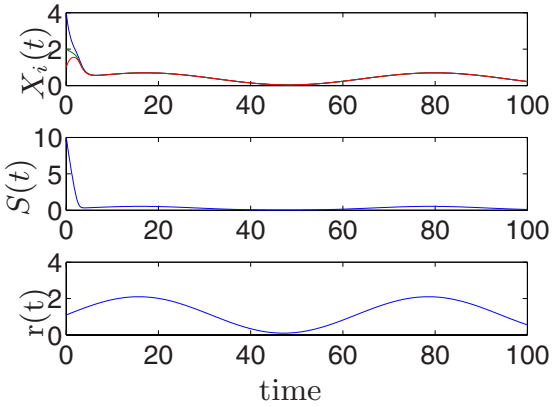

FIG. 3. (Color online) Simulation of Eq. (17), with $N=3$ and $r(t)=1.1+\sin(0.1t)$. System parameters are set as follows: $a=1$, $K_2=1$, and $K_1=2$.

$$\begin{bmatrix} -a & \dfrac{K_2}{(K_2+y_1)^2} \\ 0 & -N\dfrac{K_2}{(K_2+y_1)^2} \end{bmatrix}. \tag{19}$$

It is straightforward to check that the above matrix represents a contracting hierarchy (recall that biochemical parameters are all positive). Thus, all the trajectories of the virtual system globally exponentially converge toward a unique T-periodic solution. This, in turn, implies that X_i, $i=1,\ldots,N$, globally exponentially converges toward each other and toward the same periodic solution.

Figure 3 illustrates the behavior for $N=3$. Notice that, as expected from the above theoretical analysis, X_1, X_2, and X_3 synchronize onto a periodic orbit of the same period as $r(t)$.

V. EMERGENT PROPERTIES AS N INCREASES

In this section, we analyze how the convergence properties of a given quorum-sensing network vary as the number N of nodes increases. We show that for some typical quorum-sensing networks, as N becomes sufficiently large, synchronization always occurs. One particular modeling context where these results have important implications is that of cell proliferation in biological systems.

A. Lower bound on N ensuring synchronization

It is well known [49] that for all-to-all diffusively coupled networks of the form

$$\dot{x}_i = f(x_i,t) + \sum_{i=1}^{N} k(x_j - x_i), \tag{20}$$

the minimum coupling gain k required for synchronization is inversely proportional to the number of nodes composing the network. That is,

$$k_{\min} \propto \frac{1}{N}.$$

We now show that a similar bound holds for nodes coupled by means of quorum sensing of the form

$$\dot{x}_i = f(x_i,t) + kN(z - x_i), \quad i = 1, \ldots, N,$$

$$\dot{z} = g[z, \Psi(x_1, \ldots, x_N), t]. \tag{21}$$

To simplify notations, the above model assumes that z and all x_i have the same dimensions. In addition, the coupling strength increases with the number of nodes N, a frequent property of actual networks based on quorum-sensing mechanisms, such as, e.g., bacteria proliferation [16] or local-field potentials.

Theorem 9. Assume that the Jacobian $(\frac{\partial f}{\partial x})$ is upper bounded by α for some matrix measure μ, i.e.,

$$\exists \alpha \in \mathbb{R}, \quad \forall \ x, \quad \forall \ t \geq 0, \quad \mu\left(\frac{\partial f}{\partial x}\right) \leq \alpha.$$

Then, network (21) synchronizes if

$$k > \frac{\alpha}{N}.$$

That is, $k_{\min} \propto 1/N$.

Proof. Consider the virtual system

$$\dot{y} = f(y,t) + kN(z - y). \tag{22}$$

Synchronization is attained if the virtual system is contracting. Now, computing the matrix measure of the Jacobian in Eq. (22) yields for any x and for any $t \geq 0$,

$$\mu\left(\frac{\partial f}{\partial y} - kNI\right) \leq \mu\left(\frac{\partial f}{\partial y}\right) + kN\mu(-I) \leq \alpha - kN.$$

Thus, the virtual system is contracting if $k > \frac{\alpha}{N}$. □

B. Dependence on initial conditions

We now consider the basic quorum-sensing model (7). We derive simple conditions for the final behavior of the network to become independent of initial conditions (in the nodes and the medium) as N becomes large.

Theorem 10. Assume that for Eq. (7) the following conditions hold: (i) $\mu(\frac{\partial f}{\partial x}) \to -\infty$ as $N \to +\infty$, (ii) $g(z,v_2(t),t)$ is contracting [for any $v_2(t)$ in $\mathbb{R}^d$], and (iii) $\|\frac{\partial f}{\partial z}\|$ and $\|\frac{\partial g}{\partial v_2}\|$ are bounded for any x, z, and v_2 (where $\|\cdot\|$ is the operator norm).

Then, there exist some N^* such that for any $N \geq N^*$ all trajectories of Eq. (7) globally exponentially converge toward a unique synchronized solution, independent of initial conditions.

Proof. We know that contraction of $f(x,v_1(t),t)$ for any $v_1(t)$ (which the first condition implies for N large enough) ensures network synchronization. That is, there exists a unique trajectory, $x_s(t)$, such that, as $t \to +\infty$,

$$|x_i - x_s| \to 0, \quad \forall \ i.$$

Therefore, the final behavior is described by the following lower-dimensional system,

$$\dot{x}_s = f(x_s, z, t),$$

$$\dot{z} = g[z, \Psi(x_s), t]. \tag{23}$$

If in turn this reduced order system (23) is contracting, then its trajectories globally exponentially converge toward a unique solution, say $x_s^*(t)$, regardless of initial conditions. This will prove the theorem (similar strategies are extensively discussed in [57]).

To show that Eq. (23) is indeed contracting, compute its Jacobian matrix

$$\begin{bmatrix} \frac{\partial f}{\partial x_s} & \frac{\partial f}{\partial z} \\ \frac{\partial g}{\partial x_s} & \frac{\partial g}{\partial z} \end{bmatrix}.$$

Lemma 1 in the Appendix shows that the above matrix is contracting if there exist some strictly positive constants θ_1, θ_2 such that

$$\mu\left(\frac{\partial f}{\partial x_s}\right) + \frac{\theta_2}{\theta_1}\left\|\frac{\partial g}{\partial x_s}\right\| \quad \text{and} \quad \mu\left(\frac{\partial g}{\partial z}\right) + \frac{\theta_1}{\theta_2}\left\|\frac{\partial f}{\partial z}\right\| \tag{24}$$

are both uniformly negative definite.

Now, $\mu(\partial f/\partial x_s)$ and $\mu(\partial g/\partial z)$ are both uniformly negative by hypotheses. Furthermore, $\mu(\partial f/\partial x_s)$ tends to be $-\infty$ as N increases: since $\|\partial f/\partial z\|$ and $\|\partial g/\partial x_s\|$ are bounded, this implies that there exist some N^* such that for any $N \geq N^*$ the two conditions in Eq. (24) are satisfied. □

Also, assume that actually the dynamics f and g do not depend explicitly on time. Then, under the conditions of the above Theorem, the reduced system is both contracting and autonomous, and so it tends toward a unique equilibrium point [43]. Thus, the original system converges to a unique equilibrium, where all x_i's are equal.

In addition, note that when the synchronization rate and the contraction rate of the reduced system both increase with N, this also increases robustness [41] to variability and disturbances.

C. How synchronization protects from noise

In this section, we discuss briefly how the synchronization mechanism provided by dynamical quorum-sensing protects from noise and variability in a fashion similar to the static mechanism studied in [21]. We show that the results of [21], to which the reader is referred for details about stochastic tools, extend straightforwardly to the case where the dynamics of the quorum variables cannot be neglected or indeed may play a central part, as studied in this paper.

Assume that the dynamics of each network element x_i in Eq. (21) is subject to noise and consider, similarly to [21], the corresponding system of individual elements in Ito form,

$$dx_i = [f(x_i, t) + kN(z - x_i)]dt + \sigma dW_i, \quad i = 1, \ldots, N, \tag{25}$$

where the all-to-all coupling in [21] has been replaced by a more general quorum-sensing mechanism. The subsystems are driven by independent noise processes, and for simplicity the noise intensity σ in the equations above is assumed to be constant. We make no assumptions about noise acting directly on the dynamics of the environment or quorum vector z.

Proceeding exactly as in [21] yields similar results on the effect of noise. In particular, let $x^\bullet$ be the center of mass of the x_i, that is

$$x^\bullet = \frac{1}{N}\sum_i x_i.$$

Notice that when all the nodes are synchronized onto some common solution, say $x_s(t)$, then, by definition, $x^\bullet = x_s(t)$.

Adding up the dynamics in Eq. (25) gives

$$dx^\bullet = \frac{1}{N}\left(\sum_i f(x_i, t)\right)dt + kN(z - x^\bullet)dt + \frac{1}{N}\sum_i \sigma dW_i. \tag{26}$$

Let

$$\epsilon = f(x^\bullet, t) - \frac{1}{N}\left(\sum_{i=1}^{N} f(x_i, t)\right).$$

Note that $\epsilon = 0$ when all the nodes are synchronized.

By analogy with Eq. (25), Eq. (26) can then be written as

$$dx^\bullet = (f(x^\bullet, t) + kN(z - x^\bullet) + \epsilon)dt + \frac{1}{N}\sum_i \sigma dW_i. \tag{27}$$

Using the Taylor formula with integral remainder exactly as in [21] yields a bound on the distortion term ϵ as a function of the nonlinearity, the coupling gain k, and the number of cells N,

$$\mathbb{E}(\|\epsilon\|) \leq \lambda_{\max}\left(\frac{\partial^2 f}{\partial x^2}\right)\rho(kN),$$

where $\lambda_{\max}(\partial^2 f/\partial x^2)$ is a uniform upper bound on the spectral radius of the Hessian $\partial^2 f/\partial x^2$ and $\rho(kN) \to 0$ as $kN \to +\infty$. In particular, in Eq. (27), both the distortion term ϵ and the average noise term $\frac{1}{N}\Sigma_i \sigma dW_i$ tend to be zero as $N \to +\infty$.

Note that an additional source of noise may be provided by the environment on the quorum variables themselves. We made no assumptions above about such noise which acts directly on the dynamics of the environment or quorum vector z. How it specifically affects the common quantity z in Eq. (25) could be further studied.

Finally, note that this noise protection property, combined with quorum sensing's computational advantage (alluded to in Sec. I, see [21]) of achieving all-to-all coupling using only $2N$ connections instead of N^2 connections, may have interesting implications in terms of the recent results in [60], which show that standard deviation from nominal trajectories due to noise varies as the quartic root of the number of signaling events.

Similar results hold for the effects of bounded disturbances and dynamic variations.

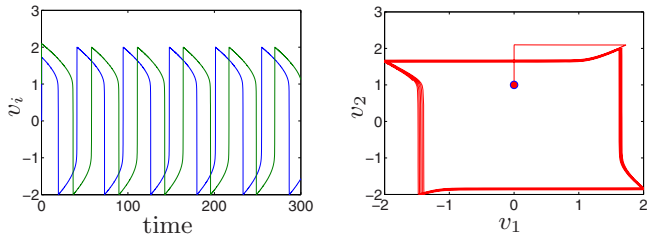

FIG. 4. (Color online) Simulation of network (28) for $N=2$, showing the absence of synchronization. Left: time behavior of v_1, v_2. Right: network phase plot, with initial conditions denoted with a round marker.

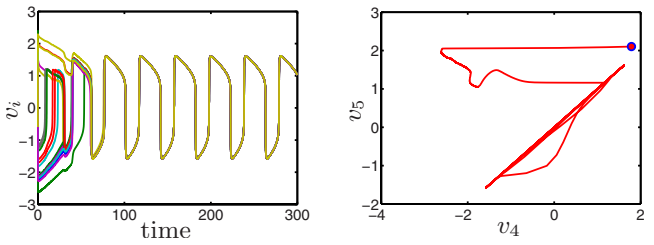

FIG. 5. (Color online) Simulation of network (28) for $N=20$, showing synchronization.

VI. EXAMPLES

A. Synchronization of the FitzHugh-Nagumo oscillators

To illustrate synchronization and population effects similar to those described in Sec. V A, consider a network of the FitzHugh-Nagumo oscillators coupled through a dynamic medium,

$$\dot{v}_i = c(v_i + w_i - 1/3v_i^3 + I) + kN(z - v_i),$$

$$\dot{w}_i = -1/c(v_i - a + bw_i),$$

$$\dot{z} = \frac{D_e}{N}\sum_{i=1}^{N}(v_i - z) - d_e z. \tag{28}$$

In what follows, system parameters are set as $a=0.3$, $b=0.2$, $c=20$, $k=1$, and $d_e=D_e=1$. Similarly to the proof of Theorem 9, consider the virtual system

$$\dot{y}_1 = c(y_1 + y_2 - 1/3y_2^3 + I) + kN(z - y_1),$$

$$\dot{y}_2 = -1/c(y_1 - a + by_2),$$

whose Jacobian matrix is

$$J := \begin{bmatrix} c(1-y_1^2) - kN & c \\ -\frac{1}{c} & -\frac{b}{c} \end{bmatrix}.$$

Using the matrix measure $\mu_{2,\Theta}$ with

$$\Theta = \begin{bmatrix} 1 & 0 \\ 0 & c \end{bmatrix}$$

yields $\mu_{2,\Theta}(J)=\mu_2(F)$, where

$$F = \Theta J \Theta^{-1} = \begin{bmatrix} c(1-y_1^2) - kN & 1 \\ -1 & -\frac{b}{c} \end{bmatrix}.$$

Thus, the virtual system is contracting if the maximum eigenvalue of the symmetric part of F is uniformly negative. Similarly to Theorem 9, this is obtained if

$$N > \frac{c}{k}. \tag{29}$$

That is, a sufficient condition for the virtual system to be contracting—and hence for network (28) to fulfill synchronization—is given in Eq. (29). Figures 4 and 5 illustrate the corresponding system behavior for values of N below and above this threshold.

B. Controlling synchronization of genetic oscillators

In Sec. IV we showed that bilateral coupling with the environment also allowed the synchronized behavior of the network nodes to be of a given period by driving the environment variable by an exogenous signal having that period. Here, we illustrate this result on a model of a population of genetic oscillators coupled by means of the concentration of a protein in the environment.

1. Genetic oscillators

Specifically, we consider the genetic circuit analyzed in [61] (a variant in [62]) and schematically represented in Fig. 6. Such a circuit is composed of two engineered gene networks that have been experimentally implemented in *E. coli*, namely, the toggle switch [63] and an intercell communication system [2]. The toggle switch is composed of two transcription factors: the *lac* repressor, encoded by gene *lacI*, and the temperature-sensitive variant of the λ*cI* repressor, encoded by the gene *cI857*. The expressions of *cI8547* and *lacI* are controlled by the promoters P_{trc} and P_{L^*}, respectively (for further details see [61]). The intercell communication

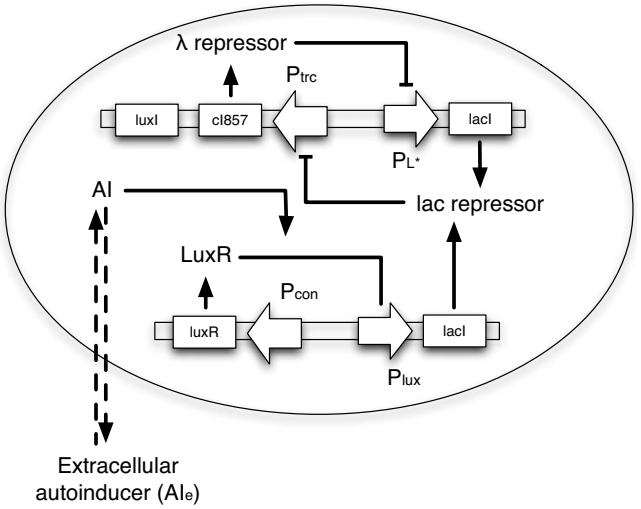

FIG. 6. A schematic representation of the genetic circuit: detailed circuit.

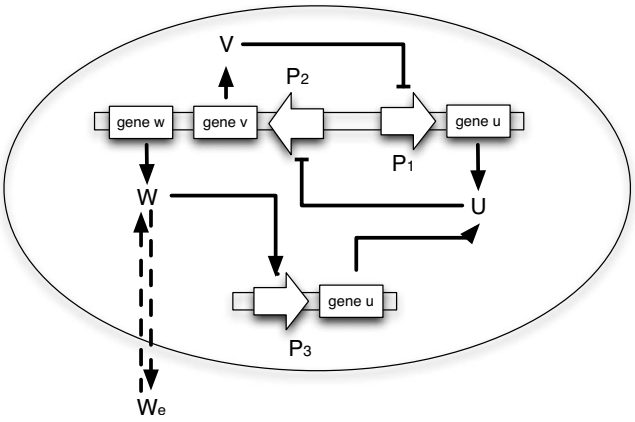

FIG. 7. Simplified circuit using for deriving mathematical model (30). Both the promoters and transcription factors are renamed.

system makes use of components of the quorum-sensing system from *Vibro fischeri* (see, e.g., [16] and references therein). Such a mechanism allows cells to sense population density through the transcription factor LuxR, which is an activator of the genes expressed by the P_{lux} promoter, when a small molecule *AI* binds to it. This small molecule, synthesized by the protein LuxI, is termed as autoinducer and it can diffuse across the cell membrane.

In [61], the following dimensionless simplified model is analyzed (see Fig. 7):

$$\dot{u}_i = \frac{\alpha_1}{1+v_i^\beta} + \frac{\alpha_3 w_i^\eta}{1+w_i^\eta} - d_1 u_i, \tag{30a}$$

$$\dot{v}_i = \frac{\alpha_2}{1+u_i^\gamma} - d_2 v_i, \tag{30b}$$

$$\dot{w}_i = \epsilon\left(\frac{\alpha_4}{1+u_i^\gamma} - d_3 w_i\right) + 2d(w_e - w_i), \tag{30c}$$

$$\dot{w}_e = \frac{D_e}{N}\sum_{i=1}^{N}(w_i - w_e) - d_e w_e, \tag{30d}$$

where u_i, v_i, and w_i denote the (dimensionless) concentrations of the *lac* repressor, λ repressor, and LuxR-AI activator, respectively. The state variable w_e denotes instead the (dimensionless) concentration of the extracellular autoinducer.

In [61], a bifurcation analysis is performed for the above model, showing that synchronization can be attained for some range of the biochemical parameters of the circuit. However, as the objective of that paper was to analyze the onset of synchronization, the problem of guaranteeing a desired oscillatory behavior was not addressed. In what follows, using the results derived in the previous sections, we address the open problem of guaranteeing a desired period for the final oscillatory behavior of network (30).

The control mechanism that we use here is an exogenous signal acting on the extracellular autoinducer concentration (see also [58]). That is, the idea is to modify Eq. (30d) as follows:

$$\dot{w}_e = \frac{D_e}{N}\sum_{i=1}^{N}(w_i - w_e) - d_e w_e + r(t), \tag{31}$$

where $r(t)$ is some T-periodic signal. In the setup that we have in mind here, multiple copies of the genetic circuit of interest share the same surrounding solution on which $r(t)$ acts. From the technological viewpoint, $r(t)$ can be implemented by controlling the temperature of the surrounding solution and/or using, e.g., the recently developed microfluidic technology (see, e.g., [64] and references therein).

In what follows, we will use Theorem 4 to find a set of biochemical parameters that ensure synchronization in Eqs. (30a)–(30d). This, using the results of Sec. IV, immediately implies that forced networks (30a)–(30c) and (31) globally exponentially converge toward a T-periodic final behavior.

System (30) has the same structure as Eq. (9), with $x_i = [u_i, v_i, w_i]^T$, $z = w_e$, and

$$f(x_i,t) = \begin{bmatrix} \dfrac{\alpha_1}{1+v_i^\beta} + \dfrac{\alpha_3 w_i^\eta}{1+w_i^\eta} - d_1 u_i \\ \dfrac{\alpha_2}{1+u_i^\gamma} - d_2 v_i \\ \epsilon\left(\dfrac{\alpha_4}{1+u_i^\gamma} - d_3 w_i\right) \end{bmatrix},$$

$$k_z(z) - k_x(x_i) = \begin{bmatrix} 0 \\ 0 \\ 2d(w_e - w_i) \end{bmatrix},$$

$$g(z,t) = -d_e w_e,$$

$$\sum_{i=1}^{N}[u_x(x_i) - u_z(z)] = \frac{D_e}{N}\sum_{i=1}^{N}(w_i - w_e).$$

We know from Theorem 7 that all nodes trajectories converge toward each other if

(1) $f(x_i,t) - k_x(x_i)$ is contracting and

(2) $g(z,t) - Nu_z(z)$ is contracting.

That is, contraction is ensured if there exist some matrix measures, μ_* and μ_{**}, such that

$$\mu_*[(x_i,t) - k_x(x_i)] \quad \text{and} \quad \mu_{**}[g(z,t) - Nu_z(z)]$$

are uniformly negative definite. We use the above two conditions in order to obtain a set of biochemical parameters ensuring node convergence. A possible choice for the above matrix measures is $\mu_* = \mu_{**} = \mu_1$ (see [65,58]). Clearly, other choices for the matrix measures μ_* and μ_{**} can be made, leading to different algebraic conditions and thus to (eventually) a different choice of biochemical parameters.

We assume that $\beta = \eta = \gamma = 2$ and show how to find a set of biochemical parameters satisfying the above two conditions.

Condition 1. Differentiation of $\partial f/\partial x_i - \partial k/\partial x_i$ yields the

Jacobian matrix (where the subscripts have been omitted),

$$J_i := \begin{bmatrix} -d_1 & \frac{-2\alpha_1 v}{(1+v^2)^2} & \frac{2\alpha_3 w}{(1+w^2)^2} \\ \frac{-2\alpha_2 u}{(1+u^2)^2} & -d_2 & 0 \\ \frac{-2\varepsilon\alpha_4 u}{(1+u^2)^2} & 0 & -\varepsilon d_3 - 2d \end{bmatrix}. \quad (32)$$

Now, by definition of μ_1, we have

$$\mu_1(J_i) = \max\left\{ -d_1 + \frac{2\alpha_2 u}{(1+u^2)^2} + \frac{2\varepsilon\alpha_4 u}{(1+u^2)^2}, -d_2 + \frac{2\alpha_1 v}{(1+v^2)^2}, -\varepsilon d_3 - 2d + \frac{2\alpha_3 w}{(1+w^2)^2} \right\}.$$

Thus, J_i is contracting if $\mu_1(J_i)$ is uniformly negative definite. That is,

$$-d_1 + \frac{2\alpha_2 u}{(1+u^2)^2} + \frac{2\varepsilon\alpha_4 u}{(1+u^2)^2} < 0,$$

$$-d_2 + \frac{2\alpha_1 v}{(1+v^2)^2} < 0,$$

$$-\varepsilon d_3 - 2d + \frac{2\alpha_3 w}{(1+w^2)^2} < 0 \quad (33)$$

uniformly. Notice now that the maximum of the function $a(v)=\bar{a}v/(1+v^2)^2$ is $\hat{a}=\frac{3\sqrt{3}\bar{a}}{16}$. Thus, the set of inequalities [Eq. (33)] is fulfilled if

$$-d_1 + \frac{6\alpha_2\sqrt{3}}{16} + \frac{6\varepsilon\alpha_4\sqrt{3}}{16} < 0,$$

$$-d_2 + \frac{6\alpha_1\sqrt{3}}{16} < 0,$$

$$-\varepsilon d_3 - 2d + \frac{6\alpha_3\sqrt{3}}{16} < 0 \quad (34)$$

uniformly.

Condition 2. In this case it is easy to check that the matrix $J_e := \frac{\partial g}{\partial z} - N\frac{\partial u}{\partial z}$ is contracting for any choice of the (positive) biochemical parameters D_e and d_e.

Thus, we can conclude that any choice of biochemical parameters fulfilling Eq. (34) ensures synchronization of the network onto a periodic orbit of period T. In [61], it was shown that a set of parameters for which synchronization is attained is $\alpha_1=3$, $\alpha_2=4.5$, $\alpha_3=1$, $\alpha_4=4$, $\varepsilon=0.01$, $d=2$, and $d_1=d_2=d_3=1$. We now use the guidelines provided by Eq. (34) to make a minimal change of the parameter values ensuring network synchronization with oscillations of period T. Specifically, such conditions can be satisfied by setting $d_1=6$, $d_2=2$. Figure 8 shows the behavior of the network for such a choice of the parameters. Finally, Figure 9 shows a simulation of the network (with $N=2$) when the biochemical parameters are chosen so as to violate the two conditions above. In such a figure, both the time behavior of w_i and phase plot are shown, indicating that synchronization is indeed not attained.

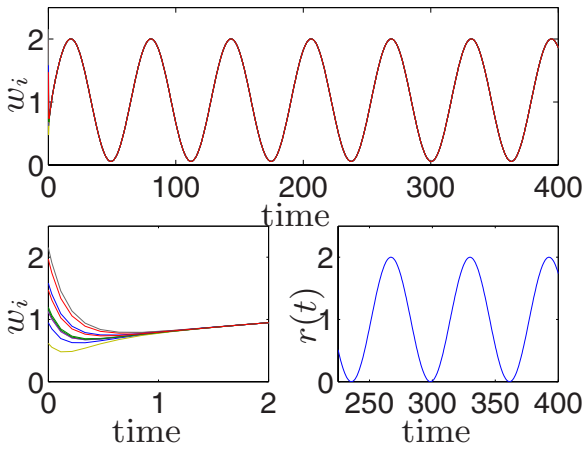

FIG. 8. (Color online) Behavior of Eqs. (30a)–(30c) and (31), when $N=10$ and $r(t)=1+\sin(0.1t)$. Notice that the nodes have initial different conditions and that they all converge (at approximately $t=2$) onto a common asymptotic having the same period as $r(t)$.

Note again that, depending on actual parameter values, the overall system may or not be contracting, and therefore synchronization to a common period is the result of coordination through the shared variable and not just of the theorem on periodic inputs of Sec. II A.

2. Communication over different media

In the above sections, we assumed that all the genetic circuits shared the same surrounding solution. We now analyze the case where two different groups of genetic circuits are surrounded by two different media. The communication between groups is then left to some (possibly artificial) communication strategy between the two media.

We now assume that only one of the two media is forced by the exogenous T-periodic signal $r(t)$, while the two media

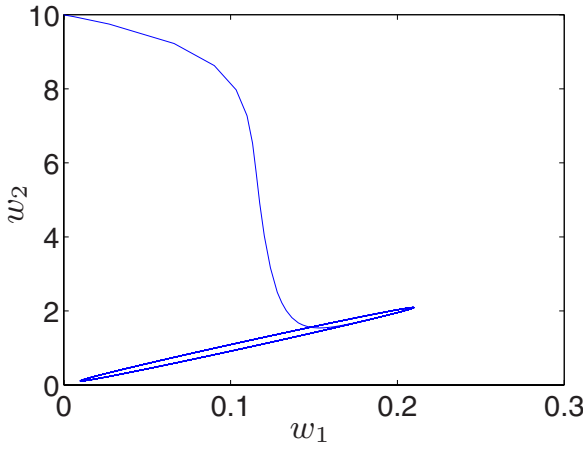

FIG. 9. (Color online) Behavior of Eqs. (30a)–(30c) and (31) when $N=2$ and all the α's are increased, violating condition 1 and condition 2. The phase plot shows that synchronization is not attained: w_1 is on the x axis and w_2 is on the y axis.

communicate with each other in a diffusive way. The mathematical model that we analyze here is then

$$\dot{u}_{i1} = \frac{\alpha_1}{1+v_{i1}^{\beta}} + \frac{\alpha_3 w_{i1}^{\eta}}{1+w_{i1}^{\eta}} - d_1 u_{i1},$$

$$\dot{v}_{i1} = \frac{\alpha_2}{1+u_{i1}^{\gamma}} - d_2 v_{i1},$$

$$\dot{w}_{i1} = \varepsilon\left(\frac{\alpha_4}{1+u_{i1}^{\gamma}} - d_3 w_{i1}\right) + 2d(w_{e1} - w_{i1}),$$

$$\dot{w}_{e1} = \frac{D_e}{N}\sum_{i=1}^{N}(w_{i1} - w_{e1}) - d_e w_{e1} + r(t) + \phi(w_{e2}) - \phi(w_{e1}),$$

$$\dot{u}_{i2} = \frac{\bar{\alpha}_1}{1+v_{i2}^{\beta}} + \frac{\bar{\alpha}_3 w_{i2}^{\eta}}{1+w_{i2}^{\eta}} - \bar{d}_1 u_{i2},$$

$$\dot{v}_{i2} = \frac{\bar{\alpha}_2}{1+u_{i2}^{\gamma}} - \bar{d}_2 v_{i2},$$

$$\dot{w}_{i2} = \varepsilon\left(\frac{\bar{\alpha}_4}{1+u_{i2}^{\gamma}} - d_3 w_{i2}\right) + 2d(w_{e2} - w_{i2}),$$

$$\dot{w}_{e2} = \frac{\bar{D}_e}{N}\sum_{i=1}^{N}(w_{i2} - w_{e2}) - \bar{d}_e w_{e2} + \phi(w_{e1}) - \phi(w_{e2}), \tag{35}$$

where $x_{i1}=[u_{i1},v_{i1},w_{i1}]^T$ and $x_{i2}=[u_{i2},v_{i2},w_{i2}]^T$ denote the set of state variables of the ith oscillator of the first and second groups, respectively. Analogously, w_{e1} and w_{e2} denote the extracellular autoinducer concentration surrounding the first and second groups of genetic circuits.

Notice that the biochemical parameters of the nodes composing the two groups and of their corresponding media are not identical. Specifically, for the first group we use the same parameters as in Sec. VI B 1, while for the second group we use parameters which differ from parameters of the first group by approximately 50% (so as to still satisfy the two conditions of Sec. VI B 1). To ensure concurrent synchronization, we design the coupling function between the media $[\phi(\cdot)]$ by using the guidelines provided by Theorem 6. Furthermore, using Theorem 8 we can conclude that the final behavior of the two groups is T periodic.

It is straightforward to check that the hypotheses of Theorem 6 are all satisfied if

(a) the biochemical parameters of the two groups fulfill the conditions in Eq. (34) and

(b) the coupling function $\phi(\cdot)$ is increasing.

In fact, the topology of the autonomous level of the network is input equivalent by construction. Figure 10 shows the behavior of Eq. (35) when the biochemical parameters of the oscillators are tuned as in Sec. VI B 1 and $\phi(x)=Kx$, with $K=0.1$.

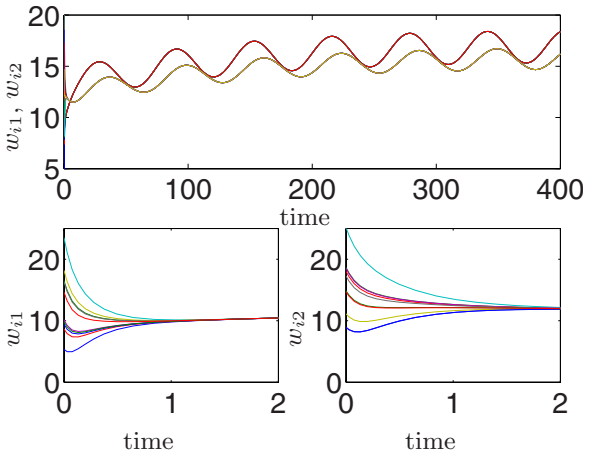

FIG. 10. (Color online) Behavior of Eq. (35) when $r(t)=1+\sin(0.1t)$. Both groups consist of $N=10$ nodes. Concurrent synchronization is attained for the network. The time behavior of the first group of nodes is in red (upper line), while the time behavior of the second group is in yellow (lower line). Both the groups exhibit a final, synchronized, behavior having the same period as $r(t)$.

3. Coexistence of multiple node dynamics

We now consider the case where the two groups analyzed above are identical but connected with each other by means of a third group composed of the Van der Pol oscillators. For such oscillators, the coupling between elements of the same group is also implemented by means of a quorum-sensing mechanism. Communication among the three groups occurs by means of some coupling between their media. The mathematical model considered here is then

$$\dot{u}_{i1} = \frac{\alpha_1}{1+v_{i1}^{\beta}} + \frac{\alpha_3 w_{i1}^{\eta}}{1+w_{i1}^{\eta}} - d_1 u_{i1},$$

$$\dot{v}_{i1} = \frac{\alpha_2}{1+u_{i1}^{\gamma}} - d_2 v_{i1},$$

$$\dot{w}_{i1} = \varepsilon\left(\frac{\alpha_4}{1+u_{i1}^{\gamma}} - d_3 w_{i1}\right) + 2d(w_{e1} - w_{i1}),$$

$$\dot{w}_{e1} = \frac{D_e}{N}\sum_{i=1}^{N}(w_{i1} - w_{e1}) - d_e w_{e1} + \phi(w_{e3}) - \phi(w_{e1}),$$

$$\dot{u}_{i2} = \frac{\alpha_1}{1+v_{i2}^{\beta}} + \frac{\alpha_3 w_{i2}^{\eta}}{1+w_{i2}^{\eta}} - d_1 u_{i2},$$

$$\dot{v}_{i2} = \frac{\alpha_2}{1+u_{i2}^{\gamma}} - d_2 v_{i2},$$

$$\dot{w}_{i2} = \varepsilon\left(\frac{\alpha_4}{1+u_{i2}^{\gamma}} - d_3 w_{i2}\right) + 2d(w_{e2} - w_{i2}),$$

$$\dot{w}_{e2} = \frac{D_e}{N}\sum_{i=1}^{N}(w_{i2} - w_{e2}) - d_e w_{e2} + \phi(w_{e3}) - \phi(w_{e2}),$$

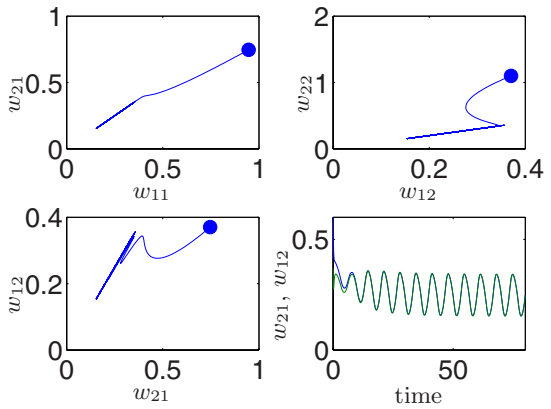

FIG. 11. (Color online) Behavior of Eq. (36): each of the two groups of genetic oscillators contains $N=4$ nodes. Top: phase plot of the nodes belonging to the first group of genetic oscillators (left) and phase plot of the nodes belonging to the second group of genetic oscillators (right). Bottom: phase plot of two nodes belonging to the two different groups of genetic oscillators (left) and their time behavior. Both the phase plots and the time series show that synchronization is attained.

$$\dot{y}_{1i} = y_{2i},$$

$$\dot{y}_{2i} = -\alpha(y_{1i}^2 - \beta)y_{2i} - \omega^2 y_{1i} + K(w_{e3} - y_{1i}),$$

$$\dot{w}_{e3} = \frac{K}{N_{vdp}} \sum_{i=1}^{N} (y_{2i} - w_{e3}) + g(w_{e3}) + \phi(w_{e1}) + \phi(w_{e2}) - 2\phi(w_{e3}), \tag{36}$$

with $[y_{1i}, y_{2i}]^T$ denoting the state variables of the ith Van der Pol oscillator and with N_{vdp} indicating the number of the Van der Pol oscillators in the network. In the above model the Van der Pol oscillators are coupled by means of the medium $w_{e3} \in \mathbb{R}$. The three media, w_{e1}, w_{e2}, and w_{e3}, communicate by means of the coupling function $\phi(\cdot)$, assumed to be linear. We assume that the function g governing the intrinsic dynamics of the medium w_{e3} is smooth with bounded derivative. The parameters for the Van der Pol oscillator are set as follows: $\alpha=\beta=\omega=1$. Notice that now no external inputs are applied on the network.

Recall that Theorem 6 ensures synchronization under the following conditions:

(1) contraction of each group composing the network and

(2) topology of the autonomous level of the network connected and input equivalent.

Notice that the second condition is satisfied for the network of our interest. Furthermore, contraction of the two groups composed of genetic oscillators is ensured if the their biochemical parameters satisfy the inequalities in Eq. (34).

To guarantee the convergent behavior of the group composed of the Van der Pol oscillators, we have to check that there exist two matrix measures, μ_* and μ_{**}, showing contraction of the following two matrices:

$$J_1 = \begin{bmatrix} 0 & 1 \\ -\alpha(y_{2i}^2 - \beta) - \omega^2 & -2\alpha y_{2i} y_{1i} - K \end{bmatrix}, \tag{37a}$$

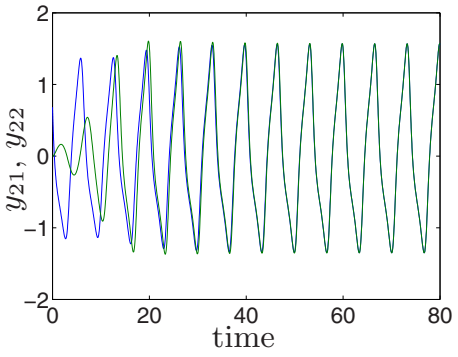

FIG. 12. (Color online) Time behavior of the two nodes composing the group of the Van der Pol oscillators in Eq. (36).

$$J_2 = \frac{\partial g}{\partial w_{e3}} - K. \tag{37b}$$

Now in [49], using the Euclidean matrix measure μ_2, it is shown that matrix (37a) is contracting if $K > \alpha$. On the other hand, to ensure contraction of J_2, we have to choose $K > \bar{G}$, where $\bar{G}$ is the maximum of $\partial g / \partial w_{e3}$. Thus, contraction of the group composed of the Van der Pol oscillators is guaranteed if the coupling gain, K, is chosen such that

$$K > \max\{\alpha, \bar{G}\}.$$

Using $g(x)=\sin(x)$, $K=2.5$, $N_{vdp}=2$, and $\phi(x)=Kx$, with $K=3$, Fig. 11 shows that all the nodes of the two groups of genetic oscillators in Eq. (36) are synchronized, in agreement with the theoretical analysis. Figure 12 also shows that the two nodes belonging to the group of the Van der Pol oscillators are synchronized with each other.

C. Analysis of a general quorum-sensing pathway

In Sec. VI B 3, we showed that our results (with appropriate choice of matrix measure) can be used to derive easily verifiable conditions on the biochemical parameters of the genetic oscillator ensuring contraction and hence synchronization (onto a periodic orbit of desired period) and concurrent synchronization. We now show that our methodology can be applied to analyze a wide class of biochemical systems involved in cell-to-cell communication.

We focus on the analysis of the pathway of the quorum-sensing mechanism that uses as autoinducers, molecules from the AHL (acyl homoserine lactone) family. The quorum-sensing pathway implemented by AHL (see Fig. 13) is one of the most common for bacteria and drives many transcriptional systems regulating their basic activities.

We now briefly describe the pathway of our interest (see [66] for further details). The enzyme LuxI produces AHL at (approximately) a constant rate. AHL in turn diffuses into and out of the cell and forms (in the cytoplasm) a complex with the receptor LuxR. Such complex polymerizes and then acts as a transcription factor by binding the DNA. This causes the increase of the production of LuxI, generating a positive feedback loop.

The pathway can be described by a set of ordinary differential equations (using the law of mass action; see [66,67]).

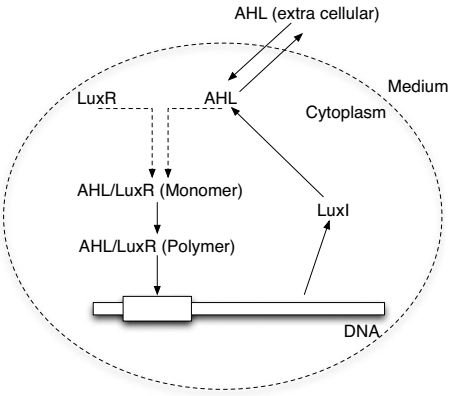

FIG. 13. The quorum-sensing pathway implemented by AHL.

Specifically, denoting with x_e the mass of AHL outside of the cell and with x_c the mass of AHL within the cell, we have the following mathematical model:

$$\dot{x}_c = \alpha + \frac{\beta x_c^n}{x_{thresh}^n + x_c^n} - \gamma_c x_c - d_1 x_c - d_2 x_e,$$

$$\dot{x}_e = d_1 x_c - d_2 x_e - \gamma_e x_e. \tag{38}$$

The physical meaning of the parameters in Eq. (38) is given in Table II.

Now, contraction of the above system is guaranteed if

(1) $-\gamma_c + 2\beta x_{thresh}^2 x_c/(x_{thresh}^2 + x_c^2)^2$ is uniformly negative definite and

(2) $-d_2 - \gamma_e$ is uniformly negative definite.

Recall that x_c and x_e are both scalars. Now, the second condition is satisfied since system parameters are all positive. That is, to prove contraction we have only to guarantee that

$$-\gamma_c + \frac{2\beta x_{thresh}^2 x_c}{(x_{thresh}^2 + x_c^2)^2}$$

is uniformly negative. Since

TABLE II. Biochemical parameters for system (38).

Parameter	Physical meaning
α	Low production rate of AHL
β	Increase of production rate of AHL
γ_c	Degradation rate of AHL in the cytosol
γ_e	Degradation rate of AHL outside the cell
d_1	Diffusion rate of the extracellular AHL
d_2	Diffusion of the intracellular AHL
x_{thresh}	Threshold of AHL between low and increased activity
n	Degree of polymerization

$$-\gamma_c + \frac{2\beta x_{thresh}^2 x_c}{(x_{thresh}^2 + x_c^2)^2} \leq -\gamma_c + \frac{3\beta\sqrt{3}}{8x_{thresh}}$$

contraction is ensured if the biochemical parameters β, g, and x_{thresh} fulfill the following condition:

$$\frac{\beta}{x_{thresh}} < \frac{8\gamma_c}{3\sqrt{3}}.$$

VII. CONCLUDING REMARKS

In this paper, we presented a systematic methodology to derive conditions for the global exponential convergence of biochemical models modeling quorum-sensing systems. To illustrate the effectiveness of our results and to emphasize the use of our techniques in synthetic biology design, we analyzed a set of biochemical networks where the quorum-sensing mechanism is involved as well as a typical pathway of the quorum sensing. In all such cases we showed that our results can be used to determine system parameters and dynamics ensuring convergence.

ACKNOWLEDGMENTS

G.R. did this work while visiting the Nonlinear Systems Laoratory, Massachusetts Institute of Technology. G.R. was supported by the European Union [FP VI NEST Project Cobious (Engineering Complexity in Biological Systems) under Grant 043379], H2CU and University of Naples Federico II.

APPENDIX: PROOFS

To prove Theorem 3 we need the following Lemma, which is a generalization of a result proven in [58].

Lemma 1. Consider the block partition for a square matrix J,

$$J = \begin{bmatrix} A(x) & B(x,y) \\ C(x,y) & D(y) \end{bmatrix},$$

where A and D are square matrices of dimensions $n_A \times n_A$ and $n_D \times n_D$, respectively. Assume that A and B are contracting with respect to μ_A and μ_D (induced by the vector norm $|\cdot|_A$ and $|\cdot|_D$). Then, J is contracting if there exists two positive real numbers θ_1, θ_2 such that

$$\mu_A(A) + \frac{\theta_2}{\theta_1}\|C(x,y)\|_{A,D} \leq -c_A^2,$$

$$\mu_D(D) + \frac{\theta_1}{\theta_2}\|B(x,y)\|_{D,A} \leq -c_B^2,$$

where $\|\cdot\|_{A,D}$ and $\|\cdot\|_{D,A}$ are the operator norms induced by $|\cdot|_A$ and $|\cdot|_D$ on the linear operators C and B. Furthermore, the contraction rate is $c^2 = \max\{c_A^2, c_B^2\}$.

Proof. Let $z := (x,y)^T$. We will show that, with the above hypotheses, J is contracting with respect to the matrix measure induced by the following vector norm:

$$|z| := \theta_1|x|_A + \theta_2|y|_D,$$

with $\theta_1, \theta_2 > 0$. In this norm, we have

$$|(I+hJ)z| = \theta_1|(I+hA)x + hBy|_A + \theta_2|(I+hD)y + hCx|_D.$$

Thus,

$$|(I+hJ)z| \le \theta_1|(I+hA)x|_A + h\theta_1|By|_{D,A} + \theta_2|(I+hD)y|_D + h\theta_2|Cx|_{A,D}.$$

Now pick $h>0$ and a unit vector z (depending on h) such that $\|(I+hJ)z\| = |(I+hJ)z|$. We have, dropping the subscripts for the norms,

$$\frac{1}{h}(\|I+hJ\|-1) \le \frac{1}{h}\left(\|I+hA\| - 1 + \frac{\theta_2}{\theta_1}h\|C\|\right)|x|\theta_1 + \frac{1}{h}\left(\|I+hD\| - 1 + \frac{\theta_1}{\theta_2}h\|B\|\right)|y|\theta_2.$$

Since $1 = |z| = \theta_1|x|_A + \theta_2|y|_B$, we finally have

$$\frac{1}{h}(\|I+hJ\|-1) \le \max\left\{\frac{1}{h}\left(\|I+hA\| - 1 + \frac{\theta_2}{\theta_1}h\|C\|\right), \frac{1}{h}\left(\|I+hD\| - 1 + \frac{\theta_1}{\theta_2}h\|B\|\right)\right\}.$$

Taking now the limit for $h \to 0^+$,

$$\mu(J) \le \max\left\{\mu(A)_A + \frac{\theta_2}{\theta_1}\|C\|, \mu(D)_D + \frac{\theta_1}{\theta_2}\|B\|\right\},$$

thus proving the result. □

Following the same arguments, Lemma 1 can be straightforwardly extended to the case of a real matrix J partitioned as

$$J = \begin{bmatrix} J_{11} & J_{12} & \dots & J_{1N} \\ \dots & \dots & \dots & \dots \\ J_{N1} & J_{N2} & \dots & J_{NN} \end{bmatrix},$$

where the diagonal blocks of J are all square matrices. Then, J is contracting if

$$\mu(J_{11}) + \frac{\theta_2}{\theta_1}\|J_{12}\| + \dots + \frac{\theta_N}{\theta_1}\|J_{1N}\| \le -c_{11}^2,$$

$$\dots$$

$$\mu(J_{NN}) + \frac{\theta_1}{\theta_N}\|J_{N1}\| + \dots + \frac{\theta_{N-1}}{\theta_N}\|J_{1N}\| \le -c_{NN}^2 \quad \text{(A1)}$$

(where subscripts for matrix measures and norms have been neglected).

Proof of Theorem 3

The assumption of input equivalence for the nodes implies the existence of a linear invariant subspace associated to the concurrent synchronization final behavior. We will prove convergence toward such a subspace by proving that the network dynamics is contracting. Let μ_f be the matrix measure where the nodes dynamics is contracting and define $X := (x_1^T, \dots, x_N^T)^T$, with $F(X)$ as the stack of all intrinsic nodes dynamics and $H(X)$ as the stack of node coupling functions. We want to prove that there exists a matrix measure, μ (which is, in general, different from μ_f), where the whole network dynamics is contracting. Denote with $L := \{l_{ij}\}$ the Laplacian matrix [68] of the network and define the matrix $\tilde{L}(X)$, whose ijth block, $\tilde{L}_{ij}(X)$, is defined as follows:

$$\tilde{L}_{ij}(X) := l_{ij}\frac{\partial h_{\gamma(i)}}{\partial x_j}.$$

[Notice that if all the nodes are identical and have the same dynamics and the same coupling functions, then $\tilde{L}$ can be written in terms of the Kronecker product, $\otimes$, as $(L \otimes I_n)\frac{\partial H}{\partial X}$, with n denoting the dimension of the nodes and I_n the $n \times n$ identity matrix.]

The Jacobian of Eq. (5) is then

$$J := \left[\frac{\partial F}{\partial X} - \tilde{L}(X)\right]. \quad \text{(A2)}$$

The system is contracting if

$$\mu\left(\frac{\partial F}{\partial X} - \tilde{L}(X)\right)$$

is uniformly negative definite. Now,

$$\mu\left[\frac{\partial F}{\partial X} - \tilde{L}(X)\right] \le \mu\left(\frac{\partial F}{\partial X}\right) + \mu[-\tilde{L}(X)].$$

Notice that, by hypotheses, the matrix $-\tilde{L}(X)$ has negative diagonal blocks and zero column sum. Thus, using Eq. (A1) with $\theta_i = \theta_j$ for all $i, j = 1, \dots, N$, $i \ne j$, yields

$$\mu[-\tilde{L}(X)] = 0.$$

Thus,

$$\mu\left(\frac{\partial F}{\partial X} - \tilde{L}(X)\right) \leq \mu\left(\frac{\partial F}{\partial X}\right).$$

Since the matrix $\frac{\partial F}{\partial X}$ is block diagonal, i.e., all of its off-diagonal elements are zero, Eq. (A1) yields

$$\mu\left(\frac{\partial F}{\partial X}\right) = \max_{x,t,i}\left\{\mu_f\left(\frac{\partial f_{\gamma(i)}}{\partial x}\right)\right\}.$$

The theorem is then proved by noticing that by hypothesis the right-hand side of the above expression is uniformly negative.

[1] S. Strogatz, *Sync: The Emerging Science of Spontaneous Order* (Hyperion, New York, 2003).
[2] L. You, R. S. Cox III, R. Weiss, and F. H. Arnold, Nature (London) **428**, 868 (2004).
[3] D. McMillen, N. Kopell, J. Hasty, and J. Collins, Proc. Natl. Acad. Sci. U.S.A. **99**, 679 (2002).
[4] H. Okamura, S. Miyake, Y. Sumi, S. Yagamuchi, A. Yasui, M. Muijtjens, J. H. J. Hoeijmakers, and G. T. J. van der Horst, Science **286**, 2531 (2003).
[5] E. Pye, Can. J. Bot. **47**, 271 (1969).
[6] A. Winfree, *The Geometry of Biological Time*, 2nd ed. (Springer, New York, 2001).
[7] M. Newman, A. Barabasi, and D. Watts, *The Structure and Dynamics of Complex Networks* (Princeton University Press, Princeton, NJ, 2006).
[8] D. Gonze, S. Bernard, C. Walterman, A. Kramer, and H. Herzerl, Biophys. J. **89**, 120 (2005).
[9] J. J. Tyson, A. Csikasz-Nagy, and B. Novak, BioEssays **24**, 1095 (2002).
[10] E. M. Izhikevich, *Dynamical Systems in Neuroscience: The Geometry of Excitability and Bursting* (MIT Press, Cambridge, MA, 2006).
[11] M. A. Henson, J. Theor. Biol. **231**, 443 (2004).
[12] E. Park, Z. Feng, and D. M. Durand, Biophys. J. **95**, 1126 (2008).
[13] A. Bohn and J. Gracia-Ojalvo, J. Theor. Biol. **250**, 37 (2008).
[14] M. Miller and B. Bassler, Annu. Rev. Microbiol. **55**, 165 (2001).
[15] C. Nadell, B. Bassler, and S. Levin, J. Biol. **7**, 27 (2008).
[16] W. Ng and B. Bassler, Annu. Rev. Genet. **43**, 197 (2009).
[17] C. Anetzberger, T. Pirch, and K. Jung, Mol. Microbiol. **73**, 267 (2009).
[18] C. D. Nadell, J. Xavier, S. A. Levin, and K. R. Foster, PLOS Comput. Biol. **6**, e14 (2008).
[19] B. Pesaran, J. Pezaris, M. Sahani, P. Mitra, and R. Andersen, Nat. Neurosci. **5**, 805 (2002).
[20] S. E. Boustani, O. Marre, P. Behuret, P. Yger, T. Bal, A. Destexhe, and Y. Fregnac, PLOS Comput. Biol. **5**, e1000519 (2009).
[21] N. Tabareau, J. Slotine, and Q. Pham, PLOS Comput. Biol. **6**, e1000637 (2010).
[22] C. Anastassiou, S. M. Montgomery, M. Barahona, G. Buzsaki, and C. Koch, J. Neurosci. **30**, 1925 (2010).
[23] M. Toiya, H. Gonzalez-Ochoa, V. K. Vanag, S. Fraden, and I. R. Epstein, The Journal of Physical Chemistry Letters **1**, 1241 (2010).
[24] M. Toiya, V. K. Vanag, and I. R. Epstein, Angew. Chem., Int. Ed. **47**, 7753 (2008).
[25] F. Fröhlich and D. A. McCormick, Neuron **67**, 129 (2010).
[26] E. Mann and O. Paulsen, Neuron **67**, 3 (2010).
[27] E. Kandel, J. Schwartz, and T. Jessel, *Principles of Neural Science*, 4th ed. (Oxford University Press, New York, 2000).
[28] E. Borenstein and S. Ullman, IEEE Trans. Pattern Anal. Mach. Intell. **30**, 2109 (2008).
[29] D. George and J. Hawkins, PLOS Comput. Biol. **5**, e1000532 (2009).
[30] G. Gigante, M. Mattia, J. Braun, and P. DelGiudice, PLOS Comput. Biol. **5**, e1000430 (2009).
[31] G. Yu and J. Slotine, IEEE Trans. Neural Netw. **20**, 1871 (2009).
[32] R. Toth, A. F. Taylor, and M. R. Tinsley, J. Phys. Chem. **110**, 10170 (2006).
[33] J. Javaloyes, M. Perrin, and A. Politi, Phys. Rev. E **78**, 011108 (2008).
[34] T. Gregor, K. Fujimoto, N. Masaki, and S. Sawai, Science **328**, 1021 (2010).
[35] A. Prindle and J. Hasty, Science **328**, 987 (2010).
[36] G. Katriel, Physica D **237**, 2933 (2008).
[37] J. Zhang, Z. Yuan, and T. Zhou, Phys. Rev. E **79**, 041903 (2009).
[38] V. Resmi, G. Ambika, and R. E. Amritkar, Phys. Rev. E **81**, 046216 (2010).
[39] J. Garcia-Ojalvo, M. B. Elowitz, and S. H. Strogatz, Proc. Natl. Acad. Sci. U.S.A. **101**, 10955 (2004).
[40] G. Russo and M. di Bernardo, J. Comput. Biol. **16**, 379 (2009).
[41] Q. C. Pham and J. J. E. Slotine, Neural Networks **20**, 62 (2007).
[42] E. Guirey, M. Bees, A. Martin, and M. Srokosz, Phys. Rev. E **81**, 051902 (2010).
[43] W. Lohmiller and J. J. E. Slotine, Automatica **34**, 683 (1998).
[44] P. Hartman, Can. J. Math. **13**, 480 (1961).
[45] D. C. Lewis, Am. J. Math. **71**, 294 (1949).
[46] A. Pavlov, A. Pogromvsky, N. van de Wouv, and H. Nijmeijer, Syst. Control Lett. **52**, 257 (2004).
[47] D. Angeli, IEEE Trans. Autom. Control **47**, 410 (2002).
[48] W. Lohmiller and J. J. Slotine, Int. J. Control **78**, 678 (2005).
[49] W. Wang and J. J. E. Slotine, Biol. Cybern. **92**, 38 (2005).
[50] G. Dahlquist, *Stability and Error Bounds in the Numerical Integration of Ordinary Differential Equations* (Transactions of the Royal Institute Technology, Stockholm, 1959).
[51] S. M. Lozinskii, Izv. Vyssh. Uchebn. Zaved., Mat. **5**, 222 (1959).
[52] J. Slotine, Int. J. Adapt. Control Signal Process. **17**, 397 (2003).
[53] M. Golubitsky, I. Stewart, and A. Torok, SIAM J. Appl. Dyn. Syst. **4**, 78 (2005).
[54] G. Russo and M. di Bernardo, *International Symposium on*

Circuits and Systems, 2009 (unpublished), pp. 305–308.
[55] S. Boccaletti, V. Latora, Y. Moreno, M. Chavez, and D. Hwang, Phys. Rep. **424**, 175 (2006).
[56] M. E. Newman, SIAM Rev. **45**, 167 (2003).
[57] S. Chung, J. Slotine, and D. Miller, J. Guid. Control Dyn. **30**, 390 (2007).
[58] G. Russo, M. di Bernardo, and E. D. Sontag, PLOS Comput. Biol. **6**, e1000739 (2010).
[59] Z. Szallasi, J. Stelling, and V. Periwal, *System Modeling in Cellular Biology: From Concepts to Nuts and Bolts* (The MIT Press, Cambridge, MA, 2006).
[60] I. Lestas, G. Vinnicombe, and J. Paulsson, Nature (London) **467**, 174 (2010).
[61] A. Kuznetsov, M. Kaern, and N. Kopell, SIAM J. Appl. Math. **65**, 392 (2004).
[62] H. Kobayashi, M. Kaern, M. Araki, K. Chung, T. Gardner, C. Cantor, and J. Collins, Proc. Natl. Acad. Sci. U.S.A. **101**, 8414 (2004).
[63] T. Gardner, C. Cantor, and J. Collins, Nature (London) **403**, 339 (2000).
[64] D. J. Beebe, G. Mensing, and G. Walker, Annu. Rev. Biomed. Eng. **4**, 261 (2002).
[65] G. Russo, M. di Bernardo, and J. Slotine, IEEE Trans. Circuits Syst., I: Regul. Pap. (to be published).
[66] J. Müller, C. Kuttler, B. Hense, M. Rothballer, and A. Hartmann, J. Math. Biol. **53**, 672 (2006).
[67] J. Dockery and J. Keener, Bull. Math. Biol. **63**, 95 (2001).
[68] C. Godsil and G. Royle, *Algebraic Graph Theory* (Springer Verlag, New York, 2001).